

Exchange splitting of the three $\bar{\Gamma}$ surface states of Ni(111) from three-dimensional spin- and angle-resolved photoemission spectroscopy

T. Okuda,^{1,2,*} J. Lobo-Checa,^{1,3} W. Auwärter,¹ M. Morscher,¹ M. Hoesch,¹ V. N. Petrov,⁴ M. Hengsberger,¹ A. Tamai,¹ A. Dolocan,¹ C. Cirelli,¹ M. Corso,¹ M. Muntwiler,¹ M. Klöckner,¹ M. Roos,⁵ J. Osterwalder,¹ and T. Greber¹

¹Physik Institut Universität Zürich, Winterthurerstrasse 190, CH 8057 Zürich, Switzerland

²The Institute for Solid State Physics, The University of Tokyo, Kashiwanoha 5-1-5, Kashiwa 277-8581, Japan

³Swiss Light Source, Paul-Scherrer-Institut, CH 5232 Villigen PSI, Switzerland

⁴St. Petersburg Technical University, 29 Polytechnicheskaya Street, St. Petersburg 195251, Russia

⁵University of Applied Sciences Winterthur, P.O. Box 805, CH 8401 Winterthur, Switzerland

(Received 2 October 2009; published 4 November 2009)

The valence-band electronic structure of a clean Ni(111) surface is investigated by spin-resolved photoemission. At room temperature the orientation of the photoelectron spins on the Bloch sphere and the exchange splitting of surface and bulk states along the surface normal ($\bar{\Gamma}$) are determined. All investigated states are found to have a sizable exchange splitting >50 meV. Since the splitting is smaller than the intrinsic line width in the spin-integrated spectrum this is only seen with a spin-resolved technique. At room-temperature photoemission reaching above the Fermi level directly shows that the Shockley type surface state S_1 has an occupied majority and an unoccupied minority band with a splitting $\Delta E_{ex}=62 \pm 15$ meV. The surface states below the Fermi energy show a larger exchange splitting for in-plane hybridization [$\Delta E_{ex}(S_3)=160$ meV] than for out-of-plane hybridization [$\Delta E_{ex}(S_2)=55$ meV].

DOI: [10.1103/PhysRevB.80.180404](https://doi.org/10.1103/PhysRevB.80.180404)

PACS number(s): 75.30.Et, 79.60.Bm, 73.20.-r

The understanding of the electron-spin dynamics at surfaces is of importance for magnetism in low dimensional systems and the realization of spintronic devices, where charge and spin polarization are transferred across interfaces.¹ In this field Ni(111) is a prominent testing ground for a ferromagnetic surface. Very early it was realized by angle-resolved photoemission that the surface has a surface state.² Later a second surface state which is exchange split and cut off by the Fermi function was found in a spin-resolved experiment.³ Only recently a related surface-state splitting was inferred from scanning tunneling spectroscopy.⁴ Though, this splitting was not present everywhere on the surface, and its Fermi vectors did not correspond to the previous inverse photoemission³ nor photoemission experiments.⁵ Also, spin-integrated state of the art high-resolution photoemission⁶ and corresponding scanning probe experiments did not resolve this issue.⁷ In particular it could not be decided whether the surface states are exchange split or not. The problem requires a spin-resolved experiment that is able to resolve spin splittings smaller than the intrinsic line width. In this Rapid Communication we clarify the experimental situation with a spin analysis of the surface states along the surface normal of Ni(111). All surface states, including the third one that was also predicted by theory,⁸ but identified only recently,⁹ are found to be exchange split, though the splitting is lower than that of the bulk states. The magnitude of the splitting depends on the symmetry of the states and gives direct insight into the surface magnetism.

Three-dimensional spin- and angle-resolved photoemission spectroscopy (SARPES) experiments were performed at the COmplete PHotoEmission Experiment (COPHEE) endstation¹⁰ at the Surface and Interface Spectroscopy (SIS) beamline at the Swiss Light Source (SLS). p -polarized light with a photon energy of 21.2 eV was used. The energy and angular resolution of the SARPES measurements are 70

meV and $\pm 0.5^\circ$. All measurements were done at room temperature with a base pressure in the 10^{-11} mbar range. The two Mott detectors of COPHEE access the three-dimensional electron-spin orientation. The two spin detectors are orthogonally arranged and allow the reconstruction of the three-dimensional Mott scattering asymmetry $\mathbf{A}=(A_x, A_y, A_z)$, with A_z being measured redundantly in each Mott detector in the laboratory frame x, y, z . In order to minimize systematic errors, e.g., due to inequalities of the eight individual electron counters in the two Mott detectors, we show spin-resolved spectra obtained from cross asymmetry data of opposite magnetizations. The cross asymmetry is $\mathbf{A}^\otimes=(\mathbf{A}^+-\mathbf{A}^-)/2$, where \mathbf{A}^+ and \mathbf{A}^- are the asymmetries obtained after positive or negative current pulses in the sample coil. The effective Sherman function S_{eff} that is needed for the extraction of the spin polarized spectra has been determined on the same Ni(111) yoke sample in assuming that the minority d bands at the Fermi level are fully polarized.¹⁰ The value of $S_{eff}=0.024 \pm 0.001$ indicates a magnetization of about 30%. The Ni(111) single crystal has yoke shape (see Fig. 1). The sample is expected to be magnetized in-plane, which is of use for the experiment that does not permit stray fields in the vacuum. Since the easy magnetization axis of nickel is along $\langle 111 \rangle$, no easy axis lies in the (111) plane. Following earlier picture frame crystal designs¹¹ the long side of the yoke has been chosen to be along a second easy $\langle 110 \rangle$ axis. Reproducible magnetization of the sample for the spin-resolved photoemission was obtained at room temperature by discharging 0.12 C from a 3 mF capacitor across the sample coil with 6 loops. The sample was cleaned by repeated cycles of Ar⁺ sputtering at 0.75 kV followed by O₂ exposure of 18 L (1.0×10^{-7} mbar \times 3 min) and subsequent annealing to 1000 K. The surface cleanliness and quality are ascertained by low-energy-electron-diffraction (LEED), x-ray photoemission spectroscopy (XPS) and confirmed by well re-

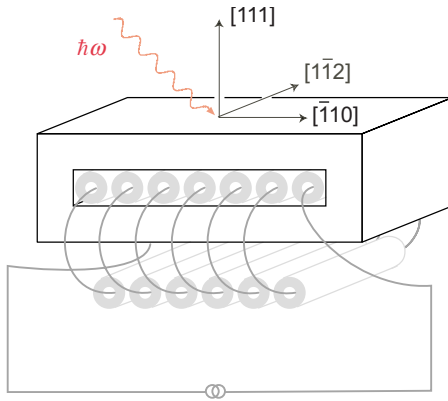


FIG. 1. (Color online) Experimental geometry. The yoke sample is cut out of a single crystal of nickel and is magnetized by current pulses across the sample coil. The $[111]$ direction is the surface normal and $[\bar{1}10]$ points along the long side of the yoke. During data taking this procedure was repeated every hour. p -polarized light $\hbar\omega=21.2$ eV with 45° incidence angle is used.

solved surface states in the ARPES spectrum. After obtaining the extremely clean surface, the contamination by residual hydrogen from the synchrotron can be removed by short annealing to 850 K and active cooling to room temperature. During data taking this procedure was repeated every hour.

Figure 2 shows results from the analysis of the Mott scattering cross asymmetry \mathbf{A}^\otimes . Here, normal-emission ($\bar{\Gamma}$) data are reported and $\mathbf{A}^\otimes(E)$ is a function of the photoelectron binding energy E . Figure 2(a) shows the spin-integrated spectrum of the clean Ni(111) surface and the three cross asymmetry components (A_x, A_y, A_z). The acquisition time for the 120 energy channels was 8 h. The main feature of the spectrum are the Λ_3 and Λ_1 bulk states. In addition to these strong bulk peaks, the three surface states labeled as S_1, S_2 and S_3 can be seen as shoulders.⁹ S_1 corresponds to the Shockley surface state that is also well known for other non-magnetic face-centered-cubic *fcc* (111) surfaces.¹² S_2 and S_3 are *d* band derived with out-of-plane and in-plane symmetry, respectively.⁹ The Mott scattering asymmetry varies within the spectrum and indicates different spin polarizations for different photoelectron energies. From a ferromagnetic sample, with a given magnetization \mathbf{M} , we expect two opposite directions parallel or antiparallel to the magnetization. If $\mathbf{A}(E_i)$ is parallel to \mathbf{M} , the majority spins dominate, if it is antiparallel, the minority spins dominate the spectrum at a given energy E_i . The asymmetries in Fig. 2(a) are displayed on a polarization map that represents the Bloch sphere, i.e., a description of all possible photoelectron spin directions [Fig. 2(b)]. The plot shows the directions of $\mathbf{A}^\otimes(E)$ in a stereographic projection, where the center of the map corresponds to spins along the surface normal, and points on the unit circle to spin directions in the plane of the Ni(111) crystal. Bright colors feature likely directions and dark unlikely directions. The direction of each energy channel i corresponds to a point in the Bloch sphere plot. Each point is weighted with the length of $\mathbf{A}^\otimes(E_i)$ and convoluted with a Gaussian with 15° full width at half maximum solid angle. Clearly, two poles are seen. The angle between the poles is 171° , which is close to what is expected for a ferromagnetic

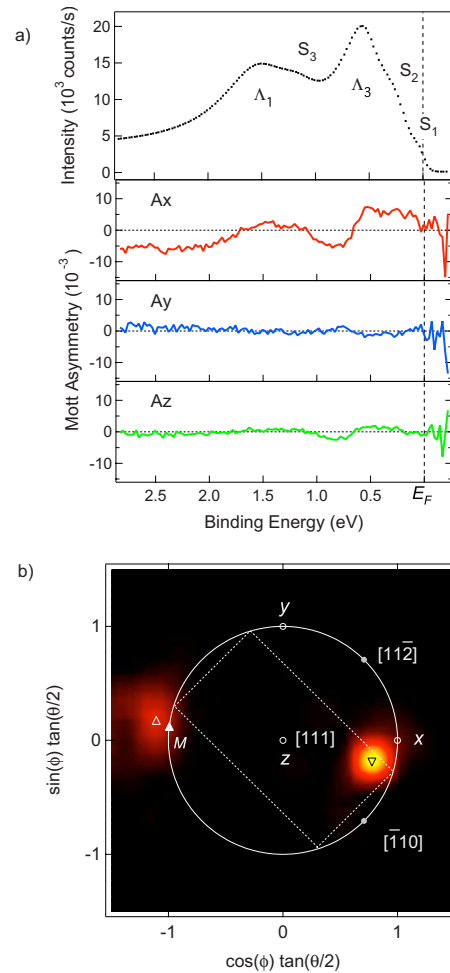


FIG. 2. (Color online) Three-dimensional Mott scattering asymmetry analysis of the Ni(111) surface. (a) Photoelectron spectrum ($\hbar\omega=21.2$ eV) recorded along the surface normal of Ni(111). The bulk bands Λ_3, Λ_1 and the three surface states S_1, S_2 , and S_3 are indicated. The Mott scattering cross asymmetry $\mathbf{A}^\otimes(E)$ is shown for the three components A_x, A_y and A_z . (b) Polarization- or Bloch sphere map, indicating the directions of $\mathbf{A}^\otimes(E)$ in stereographic projection. θ and ϕ are the polar and azimuthal angles in spherical coordinates. The center of the map ($\theta=0$) corresponds to spins pointing along the surface normal, and points on the unit circle ($\theta=\pi/2$) to spin directions in the (111) plane of the crystal. Bright colors match likely directions. Two poles (open up and down triangles) that indicate the average magnetization axis are resolved. The rectangle reproduces the top view of the yoke crystal. The white filled triangle \mathbf{M} is the magnetization direction from Ref. 13. The points x, y , and z define the laboratory reference system of the Mott detectors.

sample, where the magnetization directions are opposite, i.e., 180° apart. The two poles are near the (111) plane and lie close to the magnetization \mathbf{M} of the yoke sample, as determined in separate experiments by x-ray circular dichroism [see white filled triangle \mathbf{M} in Fig. 2(b)].¹³ From this it is seen that the magnetization does not point along the long side of the yoke that was cut along $[\bar{1}10]$ [see rectangle in Fig. 2(b)]. This is also consistent with observations on a similar yoke crystal from our group.^{10,14} The direction of the

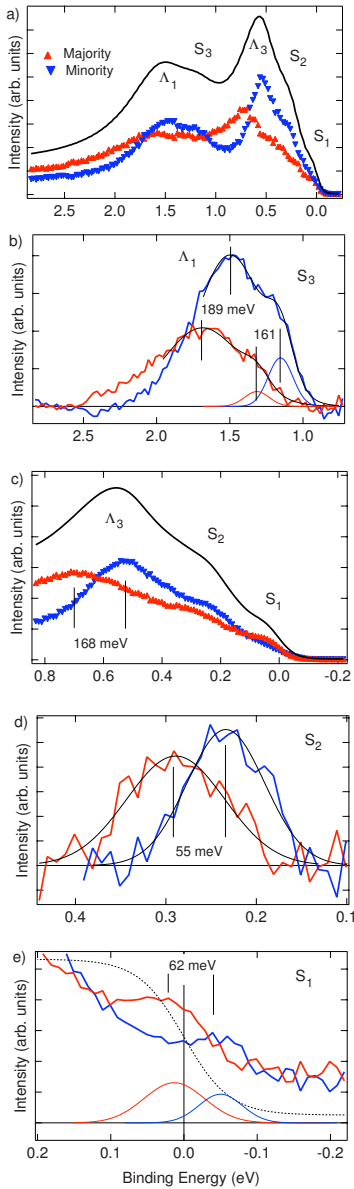


FIG. 3. (Color online) Spin-resolved photoemission from Ni(111). Normal emission, $\hbar\omega=21.2$ eV. Exchange splittings are determined by fitting Gaussians (thin solid lines) and are marked in meV. (a) Complete valence band, comprising the two bulk bands Λ_1 and Λ_3 , and the three surface states S_1 , S_2 , and S_3 . (b) Λ_1 region with S_3 . (c) Λ_3 region with S_2 and S_1 . The exchange splitting of Λ_3 is in good agreement with Ref. 15. (d) S_2 spectra after subtraction of a background. Note that the exchange splitting is smaller than the natural line width of the spin-integrated spectrum. (e) S_1 . In order to show the minority band that lies above the Fermi level, the data are normalized with a Fermi function that accounts for thermal and instrumental broadening (dotted line). Note the spin polarized photoemission above the Fermi level.

average magnetization is used in order to determine S_{eff} that is needed for the extraction of the spin polarized spectra from the data in Fig. 2(a). It also emphasizes on how important it is to know the magnetization direction for a precise spin analysis as presented in the following.

Figure 3 shows the spin-resolved photoemission spectra

of Ni(111) along the surface normal with the magnetization axis as determined from the analysis of $\mathbf{A}^{\otimes}(E)$ in Fig. 2. Figure 3(a) displays the whole valence-band spectrum with energy steps of 25 meV. It becomes apparent that the spin-up and the spin-down spectra are shifted relative to each other by about 200 meV, which is, in the Stoner picture the exchange splitting. The exchange splitting of a state X is $\Delta E_{ex}(X) = E(X^{\uparrow}) - E(X^{\downarrow})$, where X^{\uparrow} and X^{\downarrow} are the X majority (up) and minority (down) states, respectively. The splitting is, however, not constant for all five investigated bands. In Fig. 3 the Gaussian peaks from the fitting to the data are shown, and the corresponding energy positions are listed in Table I. In Fig. 3(b) the region of the Λ_1 and the recently identified S_3 band⁹ is shown. Although both, Λ_1 and S_3 are d band derived and are mainly in-plane hybridized, they do not have the same exchange splitting $\Delta E_{ex}(\Lambda_1) > \Delta E_{ex}(S_3)$. Figure 3(c) displays the Λ_3 band, S_2 and S_1 in steps of 10 meV with a compared to the data in Fig. 3(a), 1.7 times larger counting time per channel. The exchange splitting of the Λ_3 bulk bands of 168 meV is in good agreement with previous spin-resolved photoemission measurements (160 ± 20), where, however, no surface states have been observed.¹⁵ Here, the high energy- and momentum resolution together with the cleanliness of the sample resolve S_2 and S_1 in the spin-integrated and the spin-resolved data. Figure 3(d) shows the spin-resolved spectra after subtraction of a spline background with appropriate supporting intervals below and above S_2 . S_2 is exchange split, by 55 meV, though this splitting cannot be resolved by spin-integrated techniques, because it is smaller than the full width at half maximum of the spin-integrated peak. The average binding energy of S_2 (248 meV) is in full agreement with the value obtained by spin-integrated measurements.² S_2 has been proposed to be a spin-split d -like surface resonance,¹⁶ though the 20% smaller peak width of S_2^{\downarrow} with respect to S_2^{\uparrow} is an indication that S_2^{\downarrow} hybridizes stronger with bulk bands⁹ and is consistent with the predicted larger spectral weight of S_2^{\uparrow} at $\bar{\Gamma}$.¹⁷

Finally, Fig. 3(e) shows S_1 which lies close to the Fermi level. In order to see clearly the states near Fermi level, the data in Fig. 3(c) are normalized with a Fermi function and a 5% constant background that accounts for the thermal broadening and the instrumental resolution.¹⁸ For states not too far above the Fermi level, photoemission may also resolve thermally populated states.¹⁹ By the analysis, it is clear that only the majority state of S_1 is below the Fermi level, the minority state is above the Fermi level, and S_1 is exchange split by 62 ± 15 meV (see Table I). It confirms the assignment of Donath *et al.* that S_1 is an exchange-split surface state, which is cut off by the Fermi function.³ However, the present value for the exchange splitting is smaller than the 100 meV from the inverse photoemission experiments that relied on a chemical modification of the surface and an off $\bar{\Gamma}$ measurement.³ The present value for the exchange splitting coincides with a splitting as observed with STM/STS, where Braun and Rieder found surface locations with two coexistent Shockley type surface states split by 60 ± 15 meV.⁴ Notably this is the only such observation to date, where earlier²⁰ and very recent⁷ experiments found no such splitting. The STS measurements by Nishimura *et al.* do not show a 60

TABLE I. Experimentally determined photoemission binding energies and exchange splittings ΔE_{ex} in meV of electronic valence-band states of Ni(111) at room temperature, measured along the surface normal that is determined with an accuracy of $\pm 1^\circ$, with 21.2 eV photons. The errors also contain the uncertainty due to the determination of the effective Sherman function and the spline-background subtraction.

	S_1		S_2		Λ_3		S_3		Λ_1	
	This work	Previous	This work	Previous	This work	Previous	This work	Previous	This work	Previous
Spin average	-10 ± 5	94 ^a	248 ± 20	250 ^b	560 ± 15		1203 ± 10	1190 ± 80 ^c	1549 ± 15	
\uparrow_{up}	13 ± 5		289 ± 4		694 ± 6		1315 ± 19		1687 ± 8	
\downarrow_{down}	-49 ± 8		234 ± 3		526 ± 2		1154 ± 9		1498 ± 5	
ΔE_{ex}	62 ± 15	106 ± 20 ^d	55 ± 10		168 ± 10	160 ± 20 ^e	161 ± 20		189 ± 15	

^aReference 5 at 155 K.

^bReference 2.

^cReference 9.

^dReference 3.

^eReference 15.

meV splitting, instead, they also propose an occupied majority and the unoccupied minority state at 4 K, exchange split by ≈ 190 meV to display in steplike structures in the STS spectra.⁷ Our direct observation of the S_1 state with spin resolution proves the unoccupied minority and occupied majority states at room temperature. The absolute binding energies of S_1 at the band bottom ($\bar{\Gamma}$) range from 225 meV (Ref. 4) up to the Fermi level³ and this big scatter caused some confusion. It has to be noted that the binding energy of S_1 is strongly temperature dependent. This thermal shift, which is about 1 meV/K between Curie and room temperatures, reconciles data that are taken at different temperatures.²¹ Above the Curie temperature a smaller shift (0.01 meV/K), comparable to those of the nonmagnetic noble metals,²² is observed. This temperature dependence also opens the opportunity to control the density of states of the spin and the magnetic moment of the surface state²³ by temperature, where the present data suggest that S_1 is a “half metal,” i.e., has 100% spin polarization.

In conclusion, the exchange splittings of bulk and the surface states of Ni(111) are determined by spin-resolved photoemission. At room temperature the Shockley surface state S_1 is half metallic. The two d derived surface states S_2 and S_3 display an exchange splitting depending on the symmetry of the constituting d orbitals. These results provide a solid base for theories and a better understanding of the spin dynamics at a ferromagnetic surface. It should also trigger further tunneling spectroscopy experiments with spin resolution, where the scattering of differently polarized electrons can be studied on the same sample.

The authors gratefully acknowledge valuable discussions with Fabian Meier, Hugo Dil, Benjamin Braun, and Markus Donath and the hospitality of the SIS beam line team at the Swiss Light Source, where the experiments were performed. The project was funded by the Swiss National Science Foundation and TO by a Fellowship of the Ministry of Education, Culture, Sports, Science, and Technology of Japan.

*Present Address: Hiroshima Synchrotron Radiation Center, Hiroshima University, Kagamiyama 2-313, Higashi-Hiroshima 739-0046, Japan; okudat@hiroshima-u.ac.jp

¹H. C. Siegmann *J. Phys.: Condens. Matter* **4**, 8395 (1992).

²F. J. Himpsel and D. E. Eastman, *Phys. Rev. Lett.* **41**, 507 (1978).

³M. Donath, F. Passek, and V. Dose, *Phys. Rev. Lett.* **70**, 2802 (1993).

⁴K.-F. Braun and K.-H. Rieder, *Phys. Rev. B* **77**, 245429 (2008).

⁵J. Kutzner *et al.*, *Phys. Rev. B* **56**, 16003 (1997).

⁶M. Higashiguchi *et al.*, *Surf. Sci.* **601**, 4005 (2007).

⁷Y. Nishimura, M. Takeya, M. Higashiguchi, A. Kimura, M. Taniguchi, H. Narita, Y. Cui, M. Nakatake, K. Shimada, and H. Namatame, *Phys. Rev. B* **79**, 245402 (2009).

⁸D. G. Dempsey, W. R. Grise, and L. Kleinman, *Phys. Rev. B* **18**, 1550 (1978).

⁹J. Lobo-Checa, T. Okuda, M. Hengsberger, L. Patthey, T. Greber, P. Blaha, and J. Osterwalder, *Phys. Rev. B* **77**, 075415 (2008).

¹⁰M. Hoesch *et al.*, *J. Electron Spectrosc. Relat. Phenom.* **124**, 263 (2002).

¹¹M. Donath, *Surf. Sci. Rep.* **20**, 251 (1994).

¹²F. Reinert, G. Nicolay, S. Schmidt, D. Ehm, and S. Hüfner, *Phys. Rev. B* **63**, 115415 (2001).

¹³M. Morscher, F. Nolting, J. Osterwalder, and T. Greber (unpublished).

¹⁴M. Mulazzi, M. Hochstasser, J. Fujii, I. Vobornik, G. Rossi, and J. Henk, *Europhys. Lett.* **82**, 57001 (2008).

¹⁵K.-P. Kämper, W. Schmitt, and G. Güntherodt, *Phys. Rev. B* **42**, 10696 (1990).

¹⁶J. Braun and M. Donath, *Europhys. Lett.* **59**, 592 (2002).

¹⁷T. Ohwaki, D. Wortmann, H. Ishida, S. Blügel, and K. Terakura, *Phys. Rev. B* **73**, 235424 (2006).

¹⁸T. J. Kreutz, T. Greber, P. Aebi, and J. Osterwalder, *Phys. Rev. B* **58**, 1300 (1998).

¹⁹T. Greber, T. J. Kreutz, and J. Osterwalder, *Phys. Rev. Lett.* **79**, 4465 (1997).

²⁰S. Pons *et al.*, *Europhys. Lett.* **61**, 375 (2003).

²¹W. Auwärter, Ph.D. thesis, University of Zurich, 2004.

²²R. Paniago, R. Matzdorf, G. Meister, and A. Goldmann, *Surf. Sci.* **336**, 113 (1995).

²³N. Memmel, *Phys. Rev. B* **55**, 5634 (1997).